Recombination with plasmon emission in HgTe/CdHgTe multiple quantum well heterostructures

V. Ya. Aleshkin [1,2,*] and A. O. Rudakov [1,†]

[1] *Department of Semiconductor Physics, Institute for Physics of Microstructures RAS, Nizhny Novgorod 603950, Russia*

[2] *Lobachevsky State University of Nizhny Novgorod, Nizhny Novgorod 603950, Russia*

(Received 9 June 2022; revised 13 September 2022; accepted 5 October 2022; published 24 October 2022)

The work is devoted to the theoretical study of the process of recombination of nonequilibrium charge carriers with the emission of plasmons in structures with two and three quantum wells, and also in an infinite number quantum-well structure under conditions of inverse band population. The plasmon spectra in these structures have been calculated. The dependence of the average probability of electron recombination with plasmon emission on the concentration of nonequilibrium carriers for three temperatures has been found. It has been shown that an increase in the number of quantum wells leads to a slight increase in the average recombination probability.

DOI: 10.1103/PhysRevB.106.165307

I. INTRODUCTION

The problem of creating semiconductor sources of stimulated radiation in the mid-infrared (IR) range was largely solved by the advent of quantum-cascade lasers. However, quantum-cascade lasers do not work in the region of 30–45 μm [1] due to the strong phonon absorption of the material of these lasers in said region. Therefore, the search for sources of radiation generation in this region of the spectrum is an urgent task at present. One of the promising systems in which the generation of radiation in this range is possible are the HgTe/CdHgTe quantum well (QW) heterostructures. There are three main advantages of such structures. First, in such structures, it is possible to change the band gap from zero to values exceeding 1 eV by changing the parameters of the QW, which makes it possible to generate radiation in the mid-IR range [2–5]. Second, due to the features of the band structure of a narrow-gap QW, Auger recombination is suppressed there [2]. This recombination mechanism is often the main obstacle in the creation of semiconductor lasers in the mid-IR range, in which generation proceeds due to interband transitions. Third, the technology for growing such structures has been well developed by now [6,7]. The use of these advantages has led to obtaining stimulated emission from such structures in the wavelength range of 2.5–31 μm [2,8].

One of the main obstacles to the creation of interband semiconductor lasers is the processes of nonradiative recombination. The study of their features will make it possible to develop recommendations for creating the most efficient laser structures. In narrow-gap HgTe QW, recombination with the emission of two-dimensional (2D) plasmons can play an important role. Sometimes the rate of this recombination can exceed the rate of Auger recombination [9]. This recombination mechanism was previously studied in single-layer graphene [10]. However, despite the extensive study of plasmons in multilayer graphene [11,12] and other 2D materials [13,14], carrier recombination with plasmon emission has not been studied in them. This recombination mechanism was studied in structures with single HgTe quantum wells [9,15]. However, for lasers in the long-wavelength part of the IR range, as a rule, structures containing several closely spaced QWs are used, which makes it possible to increase the gain [2]. Note that there have been proposals to use HgTe QW structures to generate and amplify two-dimensional plasmons [16]. It was shown recently that multi-quantum-well (MQW) structures have some advantages over single-QW structures for the generation of two-dimensional plasmons [17].

The phenomena of recombination of nonequilibrium carriers with the emission of plasmons in MQW structures have not been studied. Filling this gap is the main task of the present work. In this paper, the probabilities of electron recombination with plasmon emission are calculated under conditions close to laser generation, when the concentrations of nonequilibrium electrons and holes are many times greater than the concentrations of equilibrium carriers.

II. CALCULATION MODEL

A. Electronic states in quantum well and plasmon dispersion relation

Consider a structure consisting of an arbitrary number of identical HgTe QWs equidistant from each other by a distance d and separated by a barrier $Cd_{0.7}Hg_{0.3}Te$ (see Fig. 1). Barriers of this compound are most often used in real HgTe/CdHgTe structures [2,3]. A plasmon with wave vector $\mathbf{q}$ and frequency ω propagates in the QW plane. To find the characteristics of plasmons, it is necessary to calculate the electron polarizability of a 2D electron gas. To calculate the polarizability, it is necessary to find the characteristics of the electron states in the QW.

To calculate the characteristics of electron states in a QW, we used the Kane model with allowance for deformation effects. The calculated spectrum of electrons in a 5-nm QW surrounded by $Cd_{0.7}Hg_{0.3}Te$ barriers is shown in Fig. 2. Note that the band gap of such a QW (35 meV) corresponds to the

*aleshkin@ipmras.ru

†rudackovartur@ipmras.ru

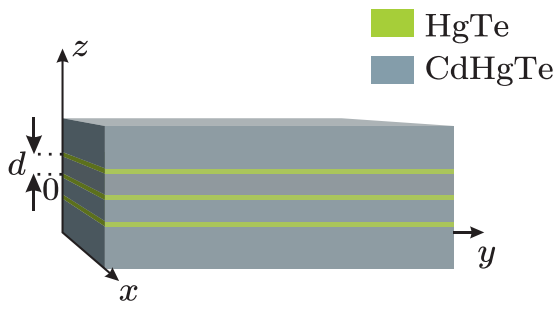

FIG. 1. Sketch of the structure under study (for example, a structure with three HgTe QWs is shown).

region of the GaAs restrahlen band. We assume in calculations that the structure under study was grown on a relaxed CdTe buffer on the (013) plane. This corresponds to experimentally studied structures [3,4]. We also assume that the distance between the QWs is much larger than the localization scale of the electron wave function. Therefore, electron tunneling between QW can be neglected, and the electron spectrum can be considered as the spectrum of electrons in each separated QW. We have neglected the effects that lead to the removal of the spin degeneracy of subbands, which are associated with a decrease in symmetry at the heterointerfaces and the absence of an inversion symmetry in the crystal lattice when we have found the states of electrons in a QW. We note that it was experimentally shown in Ref. [18] that the value of spin splitting in subbands of the conduction band of narrow-gap HgTe QWs is small. The method for calculating the electronic spectrum within the framework of this model is described in more detail in Ref. [19].

Note that, upon optical excitation when the photocarriers excited only in QWs, the carrier concentrations in different quantum wells differ only slightly due to the small absorption coefficient of light by the quantum well (∼1%) [20,21].

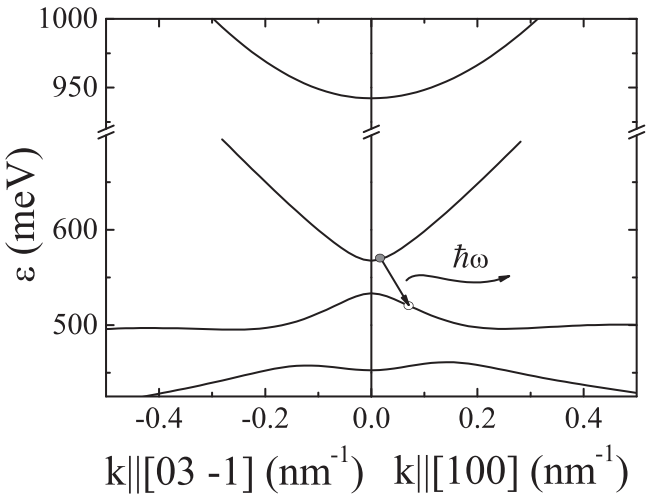

FIG. 2. Electron spectrum in a 5-nm HgTe QW surrounded with $Cd_{0.7}Hg_{0.3}Te$ barriers. The lattice temperature is $T = 4.2$ K. The straight arrow schematically shows the transition of an electron from the conduction band to the valence band with the emission of a plasmon with energy $\hbar\omega$ (wavy arrow).

Therefore, we assume the concentration of nonequilibrium carriers to be the same for all quantum wells. The position of quasi-Fermi levels in the bands was calculated at a fixed 2D concentration of nonequilibrium charge carriers n_s. To describe the distribution function of nonequilibrium carriers in subbands, we use the approximation under which nonequilibrium carriers obey the Fermi-Dirac statistics with an effective temperature T_{eff}. In the considered range of concentrations and effective temperatures, nonequilibrium electrons are located only in the lower subband of the conduction band, and nonequilibrium holes are located in the upper valence subband. Therefore, we consider only the upper subband of the valence band and the lower subband of the conduction band.

If we consider plasmons for which the product of the wave vector and the distance from the surface of the heterostructure to the nearest QW is much greater than one, then the influence of the surface on the properties of plasmons can be neglected. In this case, the medium in which the QWs are located can be considered unlimited. Obviously, in such a medium there is always a plane of symmetry. In the case of an odd number of QWs, this plane is located in the plane of the central QW, and in the case of an even number of QWs, the plane is located in the center between $N/2$ and $N/2+1$ QWs. When we are finding the plasmon spectrum, we assume that the QW thickness is much smaller than the characteristic plasmon wavelengths. Within this approximation, the polarizability of nonequilibrium carriers can be written as a sum:

$$\chi_\Sigma(\mathbf{q},\omega,z) = \chi(\mathbf{q},\omega)\sum_n \delta(z-nd), \tag{1}$$

where $\chi(\mathbf{q},\omega)$ is the polarizability of nonequilibrium carriers in a single QW HgTe, $\delta(z)$ is the Dirac delta function, n takes the values $-(N-1)/2, -(N-1)/2+1, \ldots, (N-1)/2$ (where N is the number of QWs), and d is the distance between QWs. Note that the plane $z=0$ in Eq. (1) coincides with the symmetry plane of the structure.

The polarizability of nonequilibrium carriers in a single QW with allowance for spatial dispersion can be found using the Lindhard formula [22]. We have used an approximation according to which the total polarizability of a 2D system is the sum of the polarizabilities of electrons in the conduction band and holes in the valence band, i.e., $\chi = \chi_c + \chi_v$. We neglected the interband contribution to the polarizability. By comparing the plasmon dispersions obtained in this work and the results obtained in Ref. [23] with allowance for the interband contribution to the polarizability, one can see that the interband contribution to the polarizability of electrons in a quantum well is rather small and has little effect on the plasmon dispersion law. Generalizing the Lindhard formula for the case of a finite frequency of electron scattering in a 2D electron gas [9], we obtain

$$\chi_{c,v}(\mathbf{q},\omega) = \frac{2e^2}{q^2(2\pi)^2}\int d^2k \frac{f_{c,v}(\mathbf{k}) - f_{c,v}(\mathbf{k}+\mathbf{q})}{\varepsilon_{c,v}(\mathbf{k}+\mathbf{q}) - \varepsilon_{c,v}(\mathbf{k}) - \hbar\omega - i\hbar\nu_{c,v}}, \tag{2}$$

where e is the electron charge, $f_{c,v}(\mathbf{k}) = (1+\exp[(\varepsilon_{c,v}(\mathbf{k}) - F_{c,v})/k_BT_{\text{eff}}])^{-1}$ is the Fermi-Dirac distribution function for electrons in the valence and conduction bands (k_B is the

Boltzmann constant, $F_{c,v}$ is the quasi-Fermi level in the conduction and valence bands), $\varepsilon_{c,v}(\mathbf{k})$ is the electron energy with wave vector $\mathbf{k}$ in the conduction and valence bands, $\hbar\omega$ is the plasmon energy, and $\nu_{c,v}$ is the phase relaxation frequency for the off-diagonal density matrix component. An estimate of this frequency can be obtained from the carrier mobilities $[\mu_{c,v} \approx e/(\nu_{c,v} m^*_{c,v})]$ ($m^*_{c,v}$ is the electron and hole effective masses at the Fermi level).

In a heterostructure with N QWs, there are N solutions of Maxwell's equations for plasma oscillations. If all QWs are the same, then all plasmon modes can be separated into two groups: symmetric and antisymmetric. For symmetric modes, the electric field projection onto the QW plane has the following property: $\mathbf{E}_{||}(z) = \mathbf{E}_{||}(-z)$, and for antisymmetric modes the property is $\mathbf{E}_{||}(z) = -\mathbf{E}_{||}(-z)$. Plasmons whose field component $\mathbf{E}_{||}$ does not have zeros will be referred to below as nodeless, otherwise these will be referred as nodal. From Maxwell's equations one can obtain dispersion relations for plasmons in a MQW structure. For a structure with two QWs, the dispersion relation for the symmetric plasmon mode has the following form [24–26]:

$$1 + \frac{4\pi\chi(\mathbf{q},\omega)}{\varkappa(\omega)} Q + \tanh\left(\frac{Qd}{2}\right) = 0, \tag{3}$$

and similarly for the antisymmetric mode:

$$1 + \frac{4\pi\chi(\mathbf{q},\omega)}{\varkappa(\omega)} Q + \coth\left(\frac{Qd}{2}\right) = 0, \tag{4}$$

where $\varkappa(\omega)$ is the permittivity of the barriers, $Q^2 = q^2 - \omega^2\kappa(\omega)/c^2$.

In a structure with three QWs, there are two symmetric modes and one antisymmetric mode. The dispersion relation for antisymmetric plasmon can be obtained from Eq. (4) with the change $d/2 \to d$. Symmetric modes are found from the following relations:

$$\frac{4\pi\chi}{\varkappa(\omega)} Q[1 - \exp(-2Qd)] = -2 - \exp(-2Qd) \pm \exp(-Qd)\sqrt{8 + \exp(-2Qd)}, \tag{5}$$

where the plus corresponds to the nodeless mode, and the minus corresponds to the mode with two zeros (nodes). A general method for obtaining the dispersion relations for each plasmon mode in a structure with N QWs is given in the Appendix.

A structure with an infinite number of QWs is translationally invariant along the z direction; therefore, according to Bloch's theorem, $\mathbf{E}_{||}(z + d) = \exp(iq_z d)\mathbf{E}_{||}(z)$. In such a structure, there is an infinite number of plasmon modes, each of which is characterized by a wave vector with $\mathbf{q}$ and q_z components.

The dispersion relation in such a structure was obtained in Ref. [27], and also, within the framework of the hydrodynamic model, this equation was obtained in Ref. [28]:

$$\cos(q_z d) - \cosh(Qd) - \frac{2\pi\chi}{\varkappa(\omega)} Q \sinh(Qd) = 0. \tag{6}$$

We have used the frequency dependence of the permittivity of the $Cd_{0.7}Hg_{0.3}Te$ solid solution, taken from Ref. [29], obtained from a study of reflection spectra:

$$\varkappa(\omega) = \varkappa_\infty + \sum_{j=1}^{8} \frac{S_j \omega_{Tj}^2}{\omega_{Tj}^2 - \omega^2 - i\Gamma_j\omega}; \tag{7}$$

the parameters κ_∞, S_j, ω_{Tj}, and Γ_j were taken from Ref. [29].

Calculating the polarizability of a 2D electron gas using the formula (2) and substituting it into the dispersion equations (3)–(6), one can find the plasmon spectra in MQW structures.

B. Plasmon quantization and probability of recombination with plasmon emission

Plasmons with energies exceeding the effective band gap can be emitted during the recombination of nonequilibrium carriers. The effective band gap $E_{g\,\mathrm{eff}}(q)$ equals to the minimum energy of a plasmon with the wave vector q at which it can be emitted as a result of an interband electron transition [16]. To find the probability of recombination with plasmon emission, it is necessary to quantize the plasmon field. Note that the interband electron transitions proceed mainly due to the electric field component lying in the QW plane. Since the z component of the electric field changes sign in the QW, the corresponding overlap integral is small.

In a medium with the permittivity $\widetilde{\varkappa}$, the plasmon field energy with the wave vector $\mathbf{q}$ is represented as [30]

$$\mathcal{H}_\mathbf{q} = \frac{1}{8\pi} \int d^3r \left(\frac{\partial(\omega\widetilde{\varkappa})}{\partial\omega} \overline{\mathbf{E}}_\mathbf{q}^2 + \overline{\mathbf{H}}_\mathbf{q}^2 \right), \tag{8}$$

where $\overline{\mathbf{E}}_\mathbf{q}$ and $\overline{\mathbf{H}}_\mathbf{q}$ are the period-averaged plasmon electric and magnetic fields.

It should be noted that in Refs. [9,15] a mistake was made when calculating the energy of the plasmon field—16π was written in the denominator of this formula instead of 8π. This error led to a twofold increase in the recombination probability of nonequilibrium carriers with plasmon emission.

For the permittivity in the QW plane, it is necessary to take into account the term caused by the polarization of charge carriers in the QW. The permittivity can be represented by the following expression:

$$\widetilde{\varkappa} = \begin{cases} \varkappa + 4\pi\chi \sum\limits_n \delta(z - nd) & \text{for component } \mathbf{E}_\mathbf{q} \text{ in QW plane;} \\ \varkappa & \text{for component } \mathbf{E}_\mathbf{q} \perp \text{QW plane.} \end{cases} \tag{9}$$

The expression for the electric field component of the mth plasmon mode lying in the QW plane in a system of N QWs can be written as

$$\mathbf{E}_{||}(m, \boldsymbol{r}, t) = \frac{\mathbf{q}}{q} [E_\mathbf{q} \exp(i\boldsymbol{q}\boldsymbol{\rho} - i\omega t) + E^*_\mathbf{q} \exp(-i\boldsymbol{q}\boldsymbol{\rho} + i\omega t)] f_m(z), \tag{10}$$

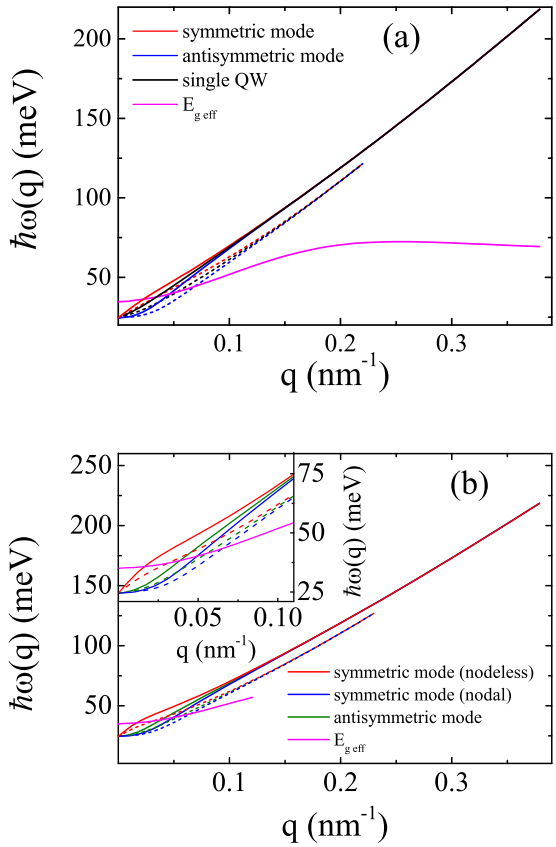

FIG. 3. Plasmon spectra in the double-QW structure (a). For comparison, the spectrum of plasmons in the single-QW structure is shown. Plasmon spectra in the triple-QW structure (b). The inset in panel (b) shows the plasmon spectra in the wave-vector interval $0 \leqslant q \leqslant 0.1$ nm^{-1} The solid lines show the plasmon spectra at a concentration $n_s = 8 \times 10^{11}$ cm^{-2}, and dashed lines correspond to $n_s = 4 \times 10^{11}$ cm^{-2}. $T_{\text{eff}} = 4.2$ K.

where $\boldsymbol{\rho}$ is the projection of the radius vector $\boldsymbol{r}$ onto the QW plane, and $f_m(z)$ is the function characterizing the dependence of the electric field of the mth plasmon mode on the coordinate z. Let us choose m so that the number of nodes in the mode equals to $m-1$. In the approximation used, the value of the z component of the electric field is also needed to calculate the energy of the plasmon field. Using Maxwell's equations, the following expression can be found for it:

$$E_z(m, \boldsymbol{r}, t) = \frac{q}{iQ^2} \frac{\partial E_{||}(m, \boldsymbol{r}, t)}{\partial z}. \tag{11}$$

In a structure with a single QW, there is only one mode ($m = 1$), and $f_1(z)$ has the form $f_1(z) = \exp(-Q|z|)$. Averaging Eq. (10) over the oscillation period and substituting it into Eq. (8), as well as neglecting the contribution of the magnetic field, we obtain the following expression for the plasmon energy in a structure with one quantum well:

$$\mathcal{H}_{\mathbf{q}}^{1\text{QW}} = |E_{\mathbf{q}}|^2 S\omega \frac{\partial \chi}{\partial \omega}, \tag{12}$$

where S is the area of the QW.

Let us estimate the contribution of the discarded term. From Maxwell's equations, the following relation is obtained: $|H(z)| = \frac{\omega\varkappa}{cq}|E_z(z)|$. Using this relation and Eq. (11), as well as the quasistatic approximation in which $Q \approx q$, we find the following estimate for the contribution of the magnetic field to the plasmon energy: $S\frac{|E_{\mathbf{q}}|^2}{q}(\frac{\omega\varkappa}{cq})^2$. The ratio of this energy to energy (12) is $(\frac{\omega\varkappa}{cq})^2(q\omega\frac{\partial\chi}{\partial\omega})^{-1}$. In order to estimate the value of $q\omega\frac{\partial\chi}{\partial\omega}$, we neglect the spatial dispersion of the polarizability and the Drude losses. In this case $q\omega\frac{\partial\chi}{\partial\omega} = -2\chi q$. From the dispersion relation for plasmons in a single-QW structure ($1 + 2\pi\chi q/\varkappa = 0$), we get the following: $-2\chi q = \varkappa/\pi$. We consider plasmons with energies greater than the energy of a longitudinal optical phonon in the barriers, since only such plasmons participate in recombination. In this case $|\varkappa| < \varkappa_\infty$, where $\varkappa_\infty$ is the high-frequency barrier permittivity. Therefore, the considered ratio is less than the value $\pi\varkappa_\infty(\frac{\omega}{cq})^2$. From Fig. 3, we can estimate the squared ratio of the phase velocities of the plasmon and the photon as $(\frac{\omega}{cq})^2 \sim 10^{-6}$. For CdHgTe $\varkappa_\infty \sim 9$, and the relation under consideration is less than 10^{-4}.

Consider a double-QW structure. In this structure, there is one symmetric mode (nodeless) and one antisymmetric mode (nodal). The function $f_m(z)$ for a symmetric plasmon has the following form:

$$f_1(z) = \begin{cases} \exp(q[z + d/2]), & z < -d/2; \\ \cosh(qz)/\cosh(qd/2), & d/2 \leqslant z \leqslant d/2; \\ \exp(-q[z - d/2]), & z > d/2; \end{cases} \tag{13}$$

and for an antisymmetric plasmon,

$$f_2(z) = \begin{cases} \exp(q[z + d/2]), & z < -d/2; \\ -\sinh(qz)/\sinh(qd/2), & d/2 \leqslant z \leqslant d/2; \\ -\exp(-q[z - d/2]), & z > d/2; \end{cases} \tag{14}$$

For both symmetric and antisymmetric plasmons in a double-QW structure, the plasmon energy has the following form:

$$\mathcal{H}_{\mathbf{q}}^{2\text{QW}} = 2|E_{\mathbf{q}}|^2 S\omega \frac{\partial \chi}{\partial \omega}. \tag{15}$$

In a triple-QW structure, there are three types of plasmons—one antisymmetric plasmon and two symmetric plasmons. For all types of plasmons, the vectors $\mathbf{E}_{||}$ on the outermost QWs in this structure are equal in absolute value. On the central QW, $\mathbf{E}_{||}$ is nonzero only for symmetric plasmons. Symmetric plasmons are represented by a nodeless mode ($m = 1$) and a two-node mode ($m = 3$). The function $f_m(z)$ for a symmetric plasmon has the following form:

$$f_{1,3}(z) = \begin{cases} \left[1 + \frac{\beta_\pm - 10}{2[1-\exp(-2qd)]}\right]\exp(-qz) - \frac{(\beta_\pm - 10)\exp(qz)}{2[1-\exp(-2qd)]}, & 0 \leqslant z \leqslant d; \\ \exp(-q[z - d]), & z > d; \end{cases} \tag{16}$$

where $\beta_\pm = 8 + \exp(-2qd) \pm \exp(-qd)\sqrt{\exp(-2qd)+8}$, β_+ corresponds to the nodeless mode ($m = 1$), and β_- corresponds to the mode with two nodes ($m = 3$).

The function $f_2(z)$ for antisymmetric plasmons in a structure with three QWs is obtained from Eq. (14) by replacing $d/2 \to d$.

In a triple-QW structure, the expression for the field energy of antisymmetric plasmons is similar to the expression (15). The energy of symmetric plasmons is equal to

$$\mathcal{H}_{\mathbf{q}}^{3\mathrm{QW}} = \frac{1}{2} S |E_{\mathbf{q}}|^2 \frac{\partial \chi}{\partial \omega} \beta_\pm. \tag{17}$$

In a structure with an infinite number of QWs, the wave-vector component q_z can be used instead of the mode number m, and then the function $f_{q_z}(z)$ is used instead of the function $f_m(z)$. If $z = 0$ corresponds to the position of the QW, then the expression for the function $f_{q_z}(z)$ in the interval $0 < z < d$ has the following form:

$$f_{q_z}(z) = \frac{\sinh[q(d-z)] - \exp(iq_z d)\sinh(qz)}{\sinh(qd)}. \tag{18}$$

Using Eq. (18), one can obtain an expression for the energy of the plasmon in a structure with an infinite number of QWs:

$$\mathcal{H}_{\mathbf{q}}^{\mathrm{MQW}} = |E_{\mathbf{q}}|^2 V \omega \frac{\partial \chi}{\partial \omega}, \tag{19}$$

where V is the volume of the structure.

Following the standard field quantization procedure [31], one can write an expression for the plasmon electric field component operator $\hat{\mathbf{E}}_{||}$ in terms of the creation and annihilation plasmon operators $\hat{c}_{\mathbf{q}}^\dagger$ and $\hat{c}_{\mathbf{q}}$. In the case of a single-QW structure, the operator of the plasmon electric field component has the following form:

$$\hat{\mathbf{E}}_{||}(m, \boldsymbol{r}, t) = \sum_{\mathbf{q}} \frac{\mathbf{q}}{q} \sqrt{\frac{\hbar}{S}\left(\frac{\partial \chi}{\partial \omega}\right)^{-1}} [\hat{c}_{\mathbf{q}} \exp(i\boldsymbol{q}\boldsymbol{\rho} - i\omega t) + \mathrm{c.c.}] f_m(z), \tag{20}$$

where c.c. is the term that is Hermitian conjugate to the first term.

For a double-QW structure the expression for the field component operator $\hat{\mathbf{E}}_{||}$ for both symmetric and antisymmetric plasmons is

$$\hat{\mathbf{E}}_{||}(m, \boldsymbol{r}, t) = \sum_{\mathbf{q}} \frac{\mathbf{q}}{q} \sqrt{\frac{\hbar}{2S}\left(\frac{\partial \chi}{\partial \omega}\right)^{-1}} [\hat{c}_{\mathbf{q}} \exp(i\boldsymbol{q}\boldsymbol{\rho} - i\omega t) + \mathrm{c.c.}] f_m(z). \tag{21}$$

In the triple-QW structure, the field amplitude at the central QW differs from the field amplitude at the outermost QWs. The expression for the operator of the plasmon electric field component $\hat{\mathbf{E}}_{||}$ has the following form:

$$\hat{\mathbf{E}}_{||}(m, \boldsymbol{r}, t) = \sum_{\mathbf{q}} \frac{\mathbf{q}}{q} \sqrt{\frac{2\hbar}{S\beta_\pm}\left(\frac{\partial \chi}{\partial \omega}\right)^{-1}} [\hat{c}_{\mathbf{q}} \exp(i\boldsymbol{q}\boldsymbol{\rho} - i\omega t) + \mathrm{c.c.}] f_m(z). \tag{22}$$

In a structure with an infinite number of QWs, $\hat{\mathbf{E}}_{||}$ in the interval $0 < z < d$ is given by

$$\hat{\mathbf{E}}_{||}(q_z, \boldsymbol{r}, t) = \sum_{\mathbf{q}} \frac{\mathbf{q}}{q} \sqrt{\frac{\hbar}{V}\left(\frac{\partial \chi}{\partial \omega}\right)^{-1}} [\hat{c}_{\mathbf{q}} \exp(i\boldsymbol{q}\boldsymbol{\rho} - i\omega t) + \mathrm{c.c.}] f_{q_z}(z), \tag{23}$$

In the jth QW, the interaction operator of an electron with an electromagnetic wave in the dipole approximation can be written as $\hat{H}_j^{int} = ie\hat{\mathbf{v}}\hat{\mathbf{E}}_{||}(z_j)/\omega$, where $\hat{\mathbf{v}}$ is the electron velocity operator, and z_j is the coordinate of the jth QW. Using the golden Fermi rule, we obtain an expression for the probability of transitions of electrons from the lth subband (l includes spin indexes) with the emission of a 2D plasmon in the jth QW:

$$W_{lj}(\mathbf{k}) = \frac{1}{\hbar\omega^2} \frac{Se^2}{2\pi} \sum_{l'} \int d^2q |\mathbf{E}_{||}(z_j) \mathbf{v}_{\mathbf{k},l;\mathbf{k}-\mathbf{q},l'}|^2 (N_{\mathbf{q}} + 1) \times \delta[\varepsilon_l(\mathbf{k}) - \varepsilon_{l'}(\mathbf{k}-\mathbf{q}) - \hbar\omega(\mathbf{q})][1 - f_{l'}(\mathbf{k}-\mathbf{q})], \tag{24}$$

where $\mathbf{v}_{\mathbf{k},l;\mathbf{k}-\mathbf{q},l'}$ is the matrix element of the velocity operator calculated between the initial state of the electron in the lth subband in the conduction band with the wave vector $\mathbf{k}$ and its final state with the wave vector $\mathbf{k} - \mathbf{q}$ in the l'th subband of the valence band, ε_l and $\varepsilon_{l'}$ are the electron energies in the initial and final states, $f_{l'}(\mathbf{k} - \mathbf{q})$ is the electron distribution function in the l'th subband of the valence band, and $N_{\mathbf{q}}$ is the plasmon occupation number.

The occupation numbers of plasmons at the chosen lattice temperature can be considered to be equal to zero. The plasmon spectrum can be assumed to be isotropic [9], so it is convenient to integrate Eq. (24) in polar coordinates. It is necessary to integrate this expression over the value of the plasmon wave vector lying in the QW plane within the range from 0 to $q_{\max}$, where $q_{\max}$ is the maximum value of the plasmon wave vector, which is determined by the onset of Landau damping. In the case of calculating the probability of recombination of nonequilibrium carriers with plasmon emission in a structure with an infinite number of QWs, it is also necessary to consider integration over the q_z components in the range from $-\pi/d$ to π/d. The expression for the recombination probability will have a form similar to Eq. (24), with the only difference being that the double integral should be replaced by a triple integral over all components of the plasmon wave vector: q_x, q_y, and q_z.

The average probability of recombination with plasmon emission in the jth QW is defined as

$$\overline{W}_j = \frac{1}{(2\pi)^2 n_s} \sum_l \int d^2k\, W_{lj}(\mathbf{k}) f_l(\mathbf{k}) = \frac{1}{(2\pi)^2 n_s} \int d^2k\, W(k) f_c(k), \tag{25}$$

where $W(k)$ is the average probability of recombination of an electron with the wave vector k. Summation in Eq. (25) is carried out only over spin indexes.

Note that in a double-QW structure the average probability of recombination with plasmon emission is the same for both

QWs, since the modules $\mathbf{E}_{||}$ are the same on each QW. For the same reason, in a triple-QW structure, the average probability of recombination with plasmon emission is the same for the edge QWs, but differs from the probability of recombination in the central QW. The average probability of nonequilibrium carrier recombination with the plasmon emission in a structure with an infinite number of QWs is the same in each QW, since the values of $\mathbf{E}_{||}$ on each QW differ by the phase factor $\exp(iq_z d)$.

III. RESULTS AND DISCUSSION

A. Plasmon dispersion relations

By numerically solving Eqs. (3)–(6), we found the dispersion plasmon relations in MQW structures, which are shown in Fig. 3. The distance d between the QWs is chosen to be 30 nm. Often similar distances between QWs have experimental structures [2,3]. The effective temperature of nonequilibrium carriers T_{eff} was assumed to be the same for electrons and holes. The phase relaxation frequency of the off-diagonal density matrix component for electrons in the conduction band, $\hbar\nu_c$, was assumed to be 1 meV, and for holes in the valence band, $\hbar\nu_v = 2$ meV. It should be noted that $\hbar\nu$ has little effect on the real part of the plasmon frequency. The lattice temperature was taken to be 4.2 K.

As the effective temperature of nonequilibrium charge carriers increases from 4.2 to 77 K, the value of $q_{\max}$ decreases due to Landau damping, which starts at lower values of the wave vectors. Figure 3 shows that an increase of the nonequilibrium carrier concentration leads to an increase of the plasmon phase velocity. The plasmon spectrum has two groups of branches: low-frequency branches and high-frequency branches, formed due to interaction with optical phonons of barriers [9,10]. The high-frequency branch of the spectrum starts from the energy of the longitudinal optical phonon in CdHgTe, while the low-frequency branch starts at the origin and at low energies its dependence is proportional to $\sqrt{q}$ [17,23]. In this work, we considered only high-frequency branches, since the energy of plasmons of the low-frequency branch is less than the effective band gap in the QW, $E_{g\,\text{eff}}(q)$. Only those plasmons whose energy is above $E_{g\,\text{eff}}(q)$ can participate in interband transitions of electrons. For this reason, plasmons of the low-frequency branches of the spectrum cannot participate in recombination.

For comparison, the plasmon dispersion spectrum in a single-QW structure is shown in Fig. 3(a) (black line). The plasmon spectrum in a single-QW structure $HgTe/Cd_{0.7}Hg_{0.3}Te$ with a width of 5 nm and a concentration of nonequilibrium charge carriers $n_s = 4 \times 10^{11}$ cm^{-2} was calculated in Ref. [9]. As the plasmon wave vector q increases, the plasmon spectra in MQW structures approach the plasmon spectrum in a single-QW structure, which can be seen from Fig. 3(a). This is explained by the fact that the plasmon fields are localized on a scale of the order of $1/q$ near each QW in the direction z. When the condition $qd \gg 1$ is satisfied, the plasmon fields correspond to the fields of noninteracting plasmons in single QWs.

Figure 4 shows the spectra of plasmons in a structure with an infinite number of QWs. It can be seen from this

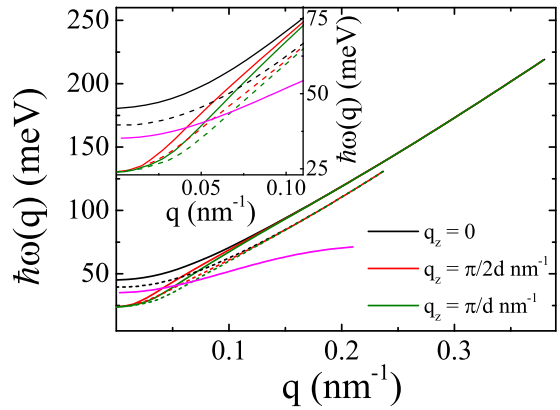

FIG. 4. Plasmon spectra in a structure with an infinite number of QWs. Solid lines show plasmon spectra at concentration $n_s = 8 \times 10^{11}$ cm^{-2}, and dashed lines show spectra at concentration $n_s = 4 \times 10^{11}$ cm^{-2}. $T_{\text{eff}} = 4.2$ K. The inset shows the plasmon spectra in the wave-vector interval $0 \leqslant q \leqslant 0.1$ nm^{-1}.

figure that the phase velocity of the plasmon decreases as the wave-vector component q_z increases. A feature of plasmons with $q_z = 0$ in a structure with an infinite number of QWs is that their spectrum starts from a certain frequency close to the "effective" plasma frequency for the chosen structure parameters [28].

It can be seen from Figs. 3 and 4 that with an increase in the concentration of nonequilibrium carriers, the value of q corresponding to the intersection of $E_{g\,\text{eff}}(q)$ and $\hbar\omega(q)$ decreases. It means that the laws of energy and momentum conservation during interband electron transitions with the plasmon emission begin to be fulfilled at lower values of q.

Figures 5 and 6 show the dependencies of the plasmon electric field component lying in the QW plane on the coordinate z in the double- and triple-QW structures for two values of the plasmon wave vector q. It can be seen from these figures that, as the plasmon wave vector increases, the field component $E_{||}$ is localized more strongly near each QW.

B. Recombination with plasmon emission

The dependencies of the average recombination probability $\overline{W}$ on the nonequilibrium charge carrier concentration n_s at two effective temperatures, 4.2 and 77 K, have been calculated by using Eq. (25) (see Fig. 7).

It can be seen from this figure that an increase in the number of QWs has little effect on the average probability of recombination with the emission of plasmons in the considered range of effective temperatures of nonequilibrium carriers. As the effective temperature of nonequilibrium carriers increases, the average probability of recombination decreases. This decrease can be due to the influence of two factors: an increase in the population of electronic states in the valence band with increasing temperature and a decrease in $q_{\max}$ due to Landau damping. To clarify the role of these factors, we present the dependence $W(k)$ in Fig. 8 calculated for different temperatures and $q_{\max}$.

For $T_{\text{eff}} = 4.2$ K we considered two cases. In the first case, we considered $q_{\max} = 0.19$ nm^{-1} (solid line in Fig. 8), this is the maximum value of the plasmon wave vector that can be

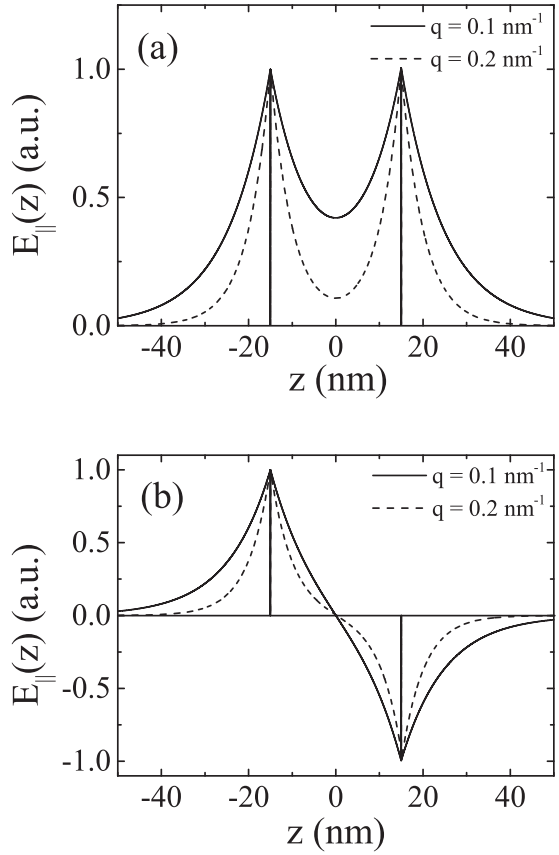

FIG. 5. Dependencies of $E_{||}(z)$ in a double-QW structure: panel (a) corresponds to the symmetric mode, and panel (b) corresponds to the antisymmetric mode.

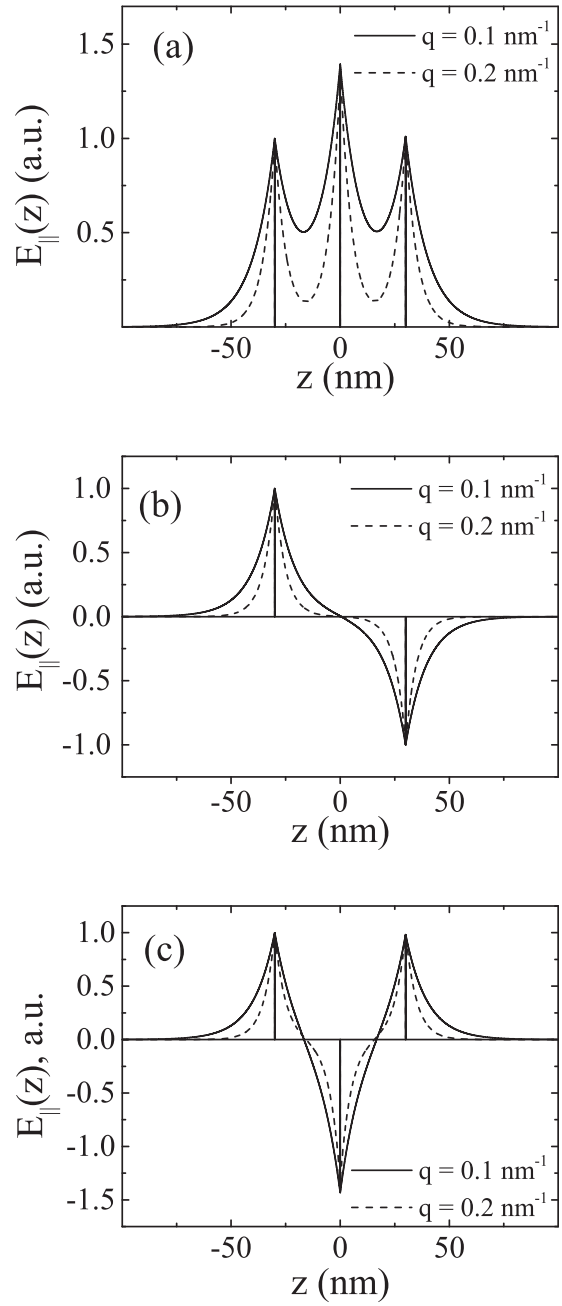

FIG. 6. Dependencies of $E_{||}(z)$ in a triple-QW structure: panel (a) corresponds to the symmetric mode (nodeless), panel (b) corresponds to antisymmetric mode, and panel (c) corresponds to the symmetric mode (nodal).

emitted during the interband electron transition at the chosen temperature and concentration of nonequilibrium carriers. In the second case, we limited $q_{\max}$ to 0.117 nm^{-1} (dashed line in Fig. 8). This value of the wave vector corresponds to the maximum value of the plasmon wave vector at the chosen concentration n_s and $T_{\text{eff}} = 77$ K. As can be seen from Fig. 8, the exclusion from consideration of plasmons whose wave vectors lie in the Landau damping region has little effect on the recombination probability. Comparing the dashed and dotted lines, it can be seen that the recombination probability decreases mainly due to an increase in the population of the final states into which electrons pass after the emission of a plasmon with an increase in the effective temperature to 77 K (dotted line in Fig. 8).

From Fig. 7(a) it can be seen that the dependence of the average probability of recombination with plasmon emission in the vicinity of a concentration equal to 3×10^{11} cm^{-2} has a maximum. A further decrease in the average probability of recombination with an increase in the concentration of nonequilibrium carriers is explained by a decrease in the "effective" density of final states in the valence band, into which electron transitions occur after the emission of plasmons. The physical meaning of the effective density of final states is that it is the totality of all states in the valence band, where an electron with a wave vector $\mathbf{k}$ transits after the emission of plasmons with all allowed wave vectors $\mathbf{q}$. The effective density of final states is represented by the following expression:

$$DoS_f(\mathbf{k}) = \frac{2}{(2\pi)^2} \int d^2q \delta[\varepsilon_c(\mathbf{k}) - \varepsilon_v(\mathbf{k}-\mathbf{q}) - \hbar\omega(\mathbf{q})]. \tag{26}$$

From Figs. 7(b) and 7(c) one can see a smooth decrease in the average recombination probability as the concentration of nonequilibrium carriers decreases from 10^{12} to 4×10^{11} cm^{-2}. The absence of a maximum at a given temperature is explained by a decrease in the occupation of the final hole

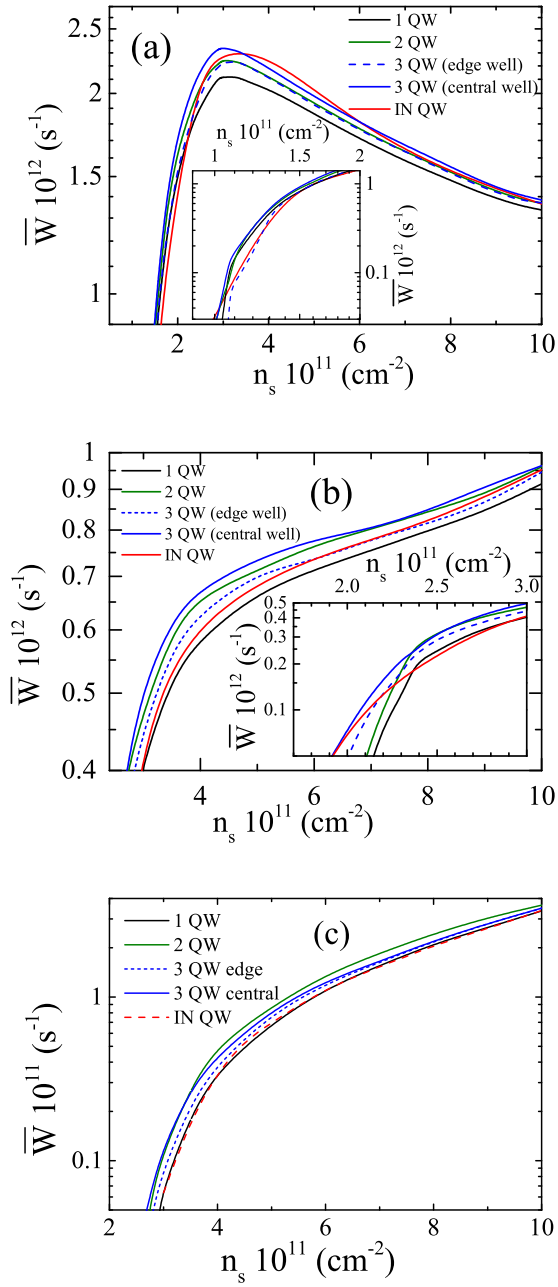

FIG. 7. Dependencies $\overline{W}(n_s)$ in the 5-nm HgTe QW: (a) $T_{\text{eff}} = 4.2$ K, (b) $T_{\text{eff}} = 77$ K, and (c) $T_{\text{eff}} = 300$ K. IN QW denotes the infinite number QW structure; insets show dependencies in the region of small $\overline{W}(n_s)$.

states, which is more pronounced at low concentrations of nonequilibrium carriers. An increase in the concentration of nonequilibrium carriers leads to an increase in the population of the final states in the valence band. Therefore, in Figs. 7(b) and 7(c) we see a gradual decrease in the average recombination probability with decreasing concentration n_s.

The rapid decrease in the average probability of recombination at concentrations approximately less than 3×10^{11} cm^{-2} ($T_{\text{eff}} = 4.2$ K) and 4×10^{11} cm^{-2} ($T_{\text{eff}} = 77$ and 300 K) is due to the fact that plasmons are "turned off" from recombination, the energies of which become lower than the

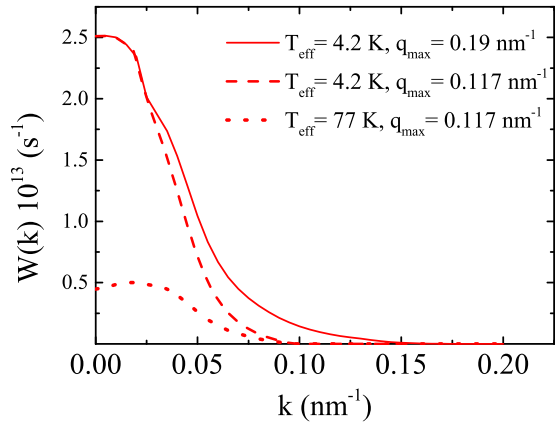

FIG. 8. Dependencies $W(k)$ for different $q_{\max}$ and T_{eff} ($n_s = 3 \times 10^{11}$ cm^{-2}).

effective band gap $E_{g\,\text{eff}}$. The laws of conservation of energy and momentum for interband transitions of electrons with the emission of plasmons with such energies are not satisfied.

IV. CONCLUSION

In conclusion, we briefly present the main results of the work.

A method is proposed for finding the dispersion relation for each plasmon mode in a structure with N QWs. Plasmon fields are quantized in structures with two, three, and an infinite number of QWs.

The dependence of the average probability of recombination with the emission of plasmons on the concentration of nonequilibrium charge carriers at effective temperatures of nonequilibrium carriers of 4.2, 77, and 300 K is calculated. It has been found that, with an increase in the number of QWs in the $HgTe/Cd_{0.7}Hg_{0.3}Te$ heterostructure, the average probability of recombination of nonequilibrium carriers with plasmon emission increases insignificantly and remains of the same order as the average probability of recombination in a structure with a single QW. At 4.2 K, the dependence of the average recombination probability on the concentration of nonequilibrium carriers is nonmonotonic and has a maximum at a concentration of nonequilibrium carriers close to 3×10^{11} cm^{-2}. With a further increase in concentration, the average recombination probability decreases due to a decrease in the effective density of hole states in the valence band, into which electrons pass after the emission of a plasmon. At 77 and 300 K, the average probability of recombination increases with an increase in the concentration of nonequilibrium carriers, since the population of hole states, into which electrons pass after they emit a plasmon, increases.

As the concentration of nonequilibrium carriers decreases approximately from 3×10^{11} cm^{-2} at 4.2 K and 4×10^{11} cm^{-2} at 77 and 300 K, the average probability of recombination with the emission of plasmons rapidly decreases due to the fact that plasmons with energies less than $E_{g\,\text{eff}}(q)$ cannot be emitted, since for these transitions with the emission of plasmons with such energies the energy and momentum conservation laws are not satisfied.

Data underlying the results presented in this paper are not publicly available at this time but may be obtained from the authors upon reasonable request.

ACKNOWLEDGMENTS

This work was supported by the Russian Science Foundation and the French Agence Nationale pour la Recherche (RSF-ANR, Grant No. 20-42-09039).

APPENDIX

The transfer matrix method can be used to calculate the plasmon dispersion relation in structures containing N QWs. The use of this method for calculating the characteristics of plasmons is discussed in detail in Refs. [32–34]. The matrix describing the propagation of $E_{||}(z)$ in the region enclosed between two neighboring QWs has the following form:

$$F = \begin{pmatrix} \exp(Qd) & 0 \\ 0 & \exp(-Qd) \end{pmatrix}. \tag{A1}$$

The matrix describing the connection of $E_{||}(z)$ to the left and to the right of a QW has the following form:

$$M = \begin{pmatrix} 1 + 2\pi\chi Q/\kappa(\omega) & 2\pi\chi Q/\kappa(\omega) \\ -2\pi\chi Q/\kappa(\omega) & 1 - 2\pi\chi Q/\kappa(\omega) \end{pmatrix}. \tag{A2}$$

In a structure with N identical QWs, the transfer matrix allows one to relate the solutions at the point $z = -(N-1)d/2 - 0$ and the point $z = -(N-1)d/2 + N + 0$. It can be represented as

$$T = (MF)^{N-1}M. \tag{A3}$$

It is easy to see that each element of the transfer matrix $T_{i,j}$, including $T_{1,1}$, is a polynomial of degree N in the variable $\frac{2\pi\chi}{\varkappa(\omega)}Q$, which can be written as

$$T_{1,1}\left(\frac{2\pi\chi}{\varkappa(\omega)}Q\right) = \sum_{n=0}^{N} c_n(d,Q)\left(\frac{2\pi\chi}{\varkappa(\omega)}Q\right)^n, \tag{A4}$$

where $c_\alpha(d,Q)$ are the polynomial coefficients. The spectra of plasmonic modes in the structure with N QWs are found from the condition $T_{11}(\frac{2\pi\chi}{\varkappa(\omega)}Q) = 0$. Polynomial (A4) has N roots for the variable $\frac{2\pi\chi}{\varkappa(\omega)}Q$, which can be denoted $X_m(d,Q)$ (m is the mode number). Having found the roots of the polynomial, the dispersion equation can be rewritten as

$$\prod_{m=1}^{N}\left(\frac{2\pi\chi}{\varkappa(\omega)}Q - X_m(d,Q)\right) = 0. \tag{A5}$$

The equality to zero of each factor (A5) is the dispersion relation for the corresponding plasmon mode.

[1] M. S. Vitiello, G. Scalari, B. Williams, and P. De Natale, Opt. Express **23**, 5167 (2015).

[2] S. V. Morozov, V. V. Rumyantsev, M. S. Zholudev, A. A. Dubinov, V. Ya. Aleshkin, V. V. Utochkin, M. A. Fadeev, K. E. Kudryavtsev, N. N. Mikhailov, S. A. Dvoretskii *et al.*, ACS Photonics **8**, 3526 (2021).

[3] V. V. Rumyantsev, A. A. Razova, L. S. Bovkun, D. A. Tatarskiy, V. Y. Mikhailovskii, M. S. Zholudev, A. V. Ikonnikov, T. A. Uaman Svetikova, K. V. Maremyanin, V. V. Utochkin *et al.*, Nanomaterials **11**, 1855 (2021).

[4] K. Kudryavtsev, V. Rumyantsev, V. Ya. Aleshkin, A. Dubinov, V. Utochkin, M. Fadeev, N. Mikhailov, G. Alymov, D. Svintsov, V. Gavrilenko *et al.*, Appl. Phys. Lett. **117**, 083103 (2020).

[5] K. Kudryavtsev, V. Rumyantsev, V. Utochkin, M. Fadeev, V. Ya. Aleshkin, A. Dubinov, M. Zholudev, N. Mikhailov, S. Dvoretskii, V. Remesnik *et al.*, J. Appl. Phys. **130**, 214302 (2021).

[6] S. Dvoretsky, N. Mikhailov, Y. Sidorov, V. Shvets, S. Danilov, B. Wittman, and S. Ganichev, J. Electron. Mater. **39**, 918 (2010).

[7] N. Mikhailov, R. Smirnov, S. Dvoretsky, Y. G. Sidorov, V. Shvets, E. Spesivtsev, and S. Rykhlitski, Int. J. Nanotechnol. **3**, 120 (2006).

[8] M. A. Fadeev, A. O. Troshkin, A. A. Dubinov, V. V. Utochkin, A. A. Razova, V. V. Rumyantsev, V. Ya. Aleshkin, V. I. Gavrilenko, N. N. Mikhailov, S. A. Dvoretsky *et al.*, Opt. Eng. **60**, 082006 (2020).

[9] V. Ya. Aleshkin, G. Alymov, A. Dubinov, V. Gavrilenko, and F. Teppe, J. Phys. Commun. **4**, 115012 (2020).

[10] F. Rana, J. H. Strait, H. Wang, and C. Manolatou, Phys. Rev. B **84**, 045437 (2011).

[11] G. Gumbs, A. Iurov, J.-Y. Wu, M. Lin, and P. Fekete, Sci. Rep. **6**, 1 (2016).

[12] O. L. Berman, R. Y. Kezerashvili, and Y. E. Lozovik, Phys. Rev. B **88**, 235424 (2013).

[13] A. Iurov, G. Gumbs, and D. Huang, J. Phys.: Condens. Matter **32**, 415303 (2020).

[14] A. Iurov, G. Gumbs, D. Huang, and L. Zhemchuzhna, J. Appl. Phys. **121**, 084306 (2017).

[15] V. Ya. Aleshkin, A. Dubinov, V. Gavrilenko, and F. Teppe, Appl. Opt. **60**, 8991 (2021).

[16] K. Kapralov, G. Alymov, D. Svintsov, and A. Dubinov, J. Phys.: Condens. Matter **32**, 065301 (2020).

[17] A. Rudakov, V. Aleshkin, and V. Gavrilenko, J. Opt. **24**, 075001 (2022).

[18] G. M. Minkov, A. V. Germanenko, O. E. Rut, A. A. Sherstobitov, M. O. Nestoklon, S. A. Dvoretski, and N. N. Mikhailov, Phys. Rev. B **93**, 155304 (2016).

[19] M. Zholudev, F. Teppe, M. Orlita, C. Consejo, J. Torres, N. Dyakonova, M. Czapkiewicz, J. Wróbel, G. Grabecki, N. Mikhailov *et al.*, Phys. Rev. B **86**, 205420 (2012).

[20] V. Ya. Aleshkin, A. Dubinov, V. Rumyantsev, M. Fadeev, O. Domnina, N. Mikhailov, S. Dvoretsky, F. Teppe, V. Gavrilenko, and S. Morozov, J. Phys.: Condens. Matter **30**, 495301 (2018).

[21] V. Ya. Aleshkin, A. Dubinov, S. Morozov, M. Ryzhii, T. Otsuji, V. Mitin, M. Shur, and V. Ryzhii, Opt. Mater. Express **8**, 1349 (2018).

[22] J. Lindhard, Dan. Vidensk. Selsk Mat.-Fys. Medd. **28**, 8 (1954).
[23] V. Ya. Aleshkin, A. Dubinov, V. Gavrilenko, and F. Teppe, J. Opt. **23**, 115001 (2021).
[24] C. H. Gan, H. S. Chu, and E. P. Li, Phys. Rev. B **85**, 125431 (2012).
[25] D. Svintsov, V. Vyurkov, V. Ryzhii, and T. Otsuji, J. Appl. Phys. **113**, 053701 (2013).
[26] M. Y. Morozov, I. Moiseenko, and V. Popov, J. Phys.: Condens. Matter **30**, 08LT02 (2018).
[27] S. Das Sarma and J. J. Quinn, Phys. Rev. B **25**, 7603 (1982).
[28] A. L. Fetter, Ann. Phys. **88**, 1 (1974).
[29] J. Polit, Bull. Pol. Acad. Sci., Tech. Sci. **59**, 331 (2011).
[30] L. D. Landau, J. Bell, M. Kearsley, L. Pitaevskii, E. Lifshitz, and J. Sykes, *Electrodynamics of Continuous Media* (Elsevier, Amsterdam, 2013), Vol. 8.
[31] L. I. Schiff, *Quantum Mechanics*, 3rd ed. (McGraw-Hill, New York, 1968).
[32] D. Smirnova, I. Iorsh, I. Shadrivov, and Y. S. Kivshar, JETP Lett. **99**, 456 (2014).
[33] A. G. Ardakani, Z. Ghasemi, and M. M. Golshan, Eur. Phys. J. Plus **132**, 1 (2017).
[34] V. Ya. Aleshkin and A. A. Dubinov, Appl. Opt. **61**, 3583 (2022).